Available online at www.sciencedirect.com
SCIENCE DIRECT
Polymer 47 (2006) 113–122
polymer
www.elsevier.com/locate/polymer

In situ polymerization approach to multiwalled carbon nanotubes-reinforced nylon 1010 composites: Mechanical properties and crystallization behavior

Hailin Zeng [a], Chao Gao [a,b,*], Yanping Wang [a,c], Paul C.P. Watts [d], Hao Kong [a], Xiaowen Cui [a], Deyue Yan [a]

[a] College of Chemistry and Chemical Engineering, Shanghai Jiao Tong University, 800 Dongchuan Road, Shanghai 200240, People's Republic of China
[b] Department of Chemistry, School of Life Sciences, Nanoscience and Nanotechnology Centre, University of Sussex, Brighton BN1 9QJ, UK
[c] State Key Laboratory for Modification of Chemical Fibre and Materials, Donghua University, Shanghai 200051, People's Republic of China
[d] Advanced Technology Centre (ATI), School of Electronics and Physical Sciences, University of Surrey, Guildford, GU2 7XH, UK

Received 30 April 2005; received in revised form 18 October 2005; accepted 1 November 2005
Available online 21 November 2005

Abstract

A series of polyamide 1010 (PA1010 or nylon 1010) and multiwalled carbon nanotubes (MWNTs) composites were prepared by in situ polymerization of carboxylic acid-functionalized MWNTs (MWNT–COOH) and nylon monomer salts. Mechanical tensile tests and dynamic mechanical analysis (DMA) show that the Young modulus increases as the content of the nanotubes increases. Compared with pure PA1010, the Young's modulus and the storage modulus of MWNTs/PA1010 in situ composites are significantly improved by ca. 87.3% and 197% (at 0 °C), respectively, when the content of MWNTs is 30.0 wt%. The elongation at break of MWNTs/PA1010 composites decreases with increasing proportion of MWNTs. For the composites containing 1.0 wt% MWNTs, the Young modulus increases by ca. 27.4%, while the elongation at break only decreases by ca. 5.4% as compared with pure PA1010 prepared under the same experimental conditions. Compared with mechanical blending of MWNTs with pure PA1010, the in situ-prepared composites exhibit a much higher Young's modulus, indicating that the in situ polycondensation method improves mechanical strength of nanocomposites. Scanning electron microscopy (SEM) imaging showed that MWNTs on the fractured surfaces of the composites are uniformly dispersed and exhibit strong interfacial adhesion with the polymer matrix. Moreover, unique crystallization and melting behaviors for MWNTs/PA1010 in situ composites are observed using a combination of differential scanning calorimetry (DSC) and X-ray diffraction methods. It was shown that only the α-form crystals are observed in our MWNTs/PA1010 in situ composites. This result is quite different from PA1010/montmorillonite and PA6-clay composites, where both of α- and γ-form crystals were found.

Keywords: Multiwalled carbon nanotubes; Nanocomposites; Nylon

1. Introduction

Accompanying the interest of nanoscience and nanotechnology, is the increased focus in the preparation of nanomaterial/polymer nanocomposites and nanohybrid materials in both academic and industrial fields. It promises an easy way to (1) improve the comprehensive properties of pure nanomaterials, and (2) design, develop and fabricate novel nanomaterials by simple chemical/physical techniques. In this regard, nanocomposites that utilize carbon nanotubes (CNTs) [1] and polymers are of particular interest. CNTs offer advantages, such as, excellent mechanical strength and high electronic and thermal conductivity. Polymeric materials present processing-ability, flexibility and can be chemically combined with CNTs [2]. Such nanocomposites can be generally prepared by melt mixing, solution processing and in situ polymerization in terms of the reaction manner [2]. They can also be prepared through the following four strategies according to the nature of interaction between CNTs and polymer (Fig. 1):

(i) non-covalent blending or mixing of CNTs with polymers;
(ii) covalent linkage of CNTs with polymers;
(iii) specific adsorption or assembly;

* Corresponding author. Address: College of Chemistry and Chemical Engineering, Shanghai Jiao Tong University, 800 Dongchuan Road, Shanghai 200240, People's Republic of China. Tel.: +86 21 54742665; fax: +86 21 54741297.
E-mail address: chaogao@sjtu.edu.cn (C. Gao).

0032-3861/$ - see front matter © 2005 Elsevier Ltd. All rights reserved.
doi:10.1016/j.polymer.2005.11.009

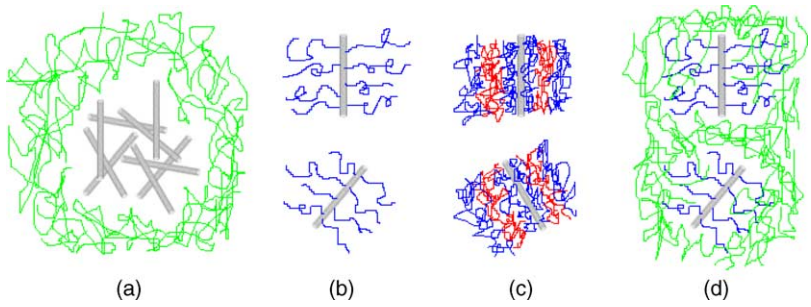

Fig. 1. Schematic illustration of CNTs dispersed mechanically in polymer matrix (a), polymer-bonded CNTs (b), polymer-coated CNTs by layer-by-layer self-assembly approach (c), and polymer-functionalized CNTs dispersed in free polymer matrix (d).

(iv) compounding previously functionalized CNTs with polymers.

Strategy (i) results in poor attraction between CNTs and the mixed polymer. Until now, direct solution [3–5], melt [6–13] and polymerization mixing methods have been employed. Direct solution and melt mixing methods are based on mixing CNTs with macromolecules. Due to entanglement, phase-aggregation and steric hindrance between macromolecules, CNT diffusion during the processing is retarded, resulting in relatively poor dispersion in the composites. Therefore, the polymerization mixing method was developed to improve CNT dispersibility. This involves initial CNT dispersal in a solution of monomer (and initiator/catalyst), and subsequent polymerization of the monomer followed by the removal of solvents [14]. Despite efforts, the dispersibility of CNTs in non-covalent systems is limited due to poor wet-ability (high surface tension), strongly associated tube bundles, and weak interaction between the tubes and polymer chains.

To address this issue, strategy (ii) was adopted and based on covalent bonding between tubes and polymers. The so-called 'grafting to' (attaching macromolecules with terminal functional groups to CNTs) and 'grafting from' (in situ polymerization of monomers in the presence of CNTs or CNT-based macroinitiators) approaches were employed to make the CNT-polymer adducts or hybrids. Hence, various linear (PS [15,16], PMMA [17], polyimide [18], poly(vinyl alcohol) (PVA) [19], poly(*m*-aminobenzene sulfonic acid) (PABS) [20], poly(sodium 4-stryrenesulfonate) [21], poly(*N*-isopropyl acrylamide) [22], poly(4-vinylpyridine) [23] and poly(*N*-vinylcarbazole) [24]) and highly branched polymers (poly(3-ethyl-3-hydroxymethyloxetane) [25], poly(amidoamine) [26] and dendrons [27]) have been successfully grafted onto CNT surfaces by the 'grafting to' or 'grafting from' approach. After the polymer is grafted to the CNTs, the resulting nanohybrids show good solubility and dispersibility in solvents, especially for adducts coated with a high density of polymer. In these cases, the CNTs are shortened to several micrometers or hundreds of nanometers, and are individually separated from each other. Consequently, individual core-shell nanocables composed of a carbon nanotube core and polymer shell can be attained [17,25]. There is little doubt that covalent functionlization of CNTs presents an important route for the design, synthesis and application of CNT-based nanomaterials and nanodevices. However, large-scale availability of these hybrid materials remains a challenge.

Strategy (iii) introduces new methods for the functionalization of CNTs as well as the preparation of CNT/polymer composites, based on specific interactions like π–π stacking [28–31], π-charge [32–34] and charge–charge attractions [21,35–39] or supramolecular assembly [21b,39,40] of polymers on the surface of CNTs. Obviously, this strategy was based on the 'specific' interaction and is only effective for compounds which can show 'specific' action with CNTs.

Strategy (iv) presents an alternate route for the preparation of CNTs/polymer composites by utilizing functionalized CNTs, and satisfies both requirements for good dispersibility and large-scale synthesis. The nature of this strategy is defined by the polymer chains, which are covalently linked to the CNT surface (or anchored polymer chains), while other polymer chains are free in the composites. The anchored polymer ensures good dispersibility, and the free polymer fraction is controllable, affording an easily tunable CNT:polymer weight ratio.

In this strategy, three methods can be utilized. Firstly, there is condensation compounding, in which oxidized or other functionalized CNTs are reacted with macromolecules by amidation [41–43] and other reactions [7,30,44]. As mentioned before, such a reaction and dispersion is limited because of the macromolecular effect. Nevertheless, it exhibited better performance as compared to strategy (i), as demonstrated by several groups. Secondly, there is mix compounding, from which polymer-grafted CNTs are mechanically mixed with pure polymer. Using this method, Sun et al. [18] prepared CNT-polyimide/polyimide composites with excellent CNT dispersion, due to dissolution of the polyimide-functionalized CNTs with a pure polyimide solution, and followed by evaporation of the solvent. Thirdly, there is polymerization compounding, in which polymer chains can be either tethered to functionalized CNTs or be free in the solution during the polymerization of the monomer. Due to the higher mobility of the monomer compared to that of macromolecules, the dispersion of CNTs in the 'polymerization compounding' nanocomposites are expected to be better than that in 'condensation compounding' nanocomposites, therefore better mechanical and other properties are expected. However, there

are few reports using this method, which will be addressed and discussed in this paper.

The primary aim of this work is to prepare CNTs/polymer composites by the polymerization compounding (or in situ polymerization) method, followed by investigation of their mechanical and thermal properties. Considering polyamide 1010 (PA1010 or nylon 1010) as an important engineering plastic due to high intensity, elasticity, toughness and abrasive resistance (but poor module [45]), we focus on CNTs/PA1010 composites herein. Multiwalled carbon nanotubes (MWNTs) were initially functionalized using a solution of sulphuric acid and nitric acid in order to introduce carboxylic acid groups on the tube surfaces. The MWNTs/PA1010 composites were then prepared by the polymerization compounding method (i.e. polymerization of PA1010's monomer salts in the presence of the oxidized MWNTs). In order to evaluate the mechanical performance of the composites, MWNTs/PA1010 composites, made by the 'blending' or 'condensation compounding' methods, were obtained for comparison.

2. Experimental section

2.1. Materials

PA1010 monomer salts and commercial PA1010 (CPA1010, type: PA1010–12, viscosity number: >116, relative density: 1.04) salts were purchased from Shanghai Celluloid Factory (China). Chemical-vapour deposition (CVD) synthesized-MWNTs were purchased from Tsinghua-Nanfine Nano-Powder Commercialization Engineering Centre.

2.2. Preparation of MWNT–COOH from MWNTs [46]

Carboxylic acid-functionalized MWNTs (MWNT–COOH) were prepared as follows: in a typical experiment, 10.078 g of crude MWNTs were added to a 200 mL mixture of concentrated sulfuric and nitric acids (volume 3:1, 98 and 60%, respectively). The mixture were ultrasonicated (40 kHz) for 30 min, and then stirred at 135 °C for 2 h under reflux. The mixture was then vacuum-filtered through 0.22 μ. Millipore polycarbonate membrane, and washed with distilled water until the pH value of the filtrate was ca. 7. The filtered solid was dried under vacuum for 12 h at 60 °C, affording 5.766 g of MWNT–COOH.

2.3. Preparation of MWNTs/PA1010 composites by in situ polymerization

Typically (a sample of NTPA-10 preparation in Table 1), PA1010 monomer salts (36 g) were put into a 100 mL flask. The flask was then placed under vacuum and crushed with high purity nitrogen thrice to remove any air. The monomer salts were mechanically stirred and heated to 190 °C under a nitrogen atmosphere for 2 h. Then, MWNT–COOH (as-prepared, 4 g) were added to the flask, and the nitrogen flow was stopped. The mixture was vigorously stirred and reacted under vacuum for 4 h at 225 °C, yielding the MWNTs/PA1010 composites (NTPA-10).

2.4. Preparation of MWNTs/PA1010 composites by melt mixing of PA1010 and MWNT–COOH

MWNTs/PA1010 blending composites with various MWNTs loadings (5.0–30.0 wt%) were prepared via the melt-mixing method using a Hacker twin-screw mixer at 220 °C for 8 min with a screw speed of 100 rpm.

2.5. Preparation of LPA1010

PA1010 monomer salts (30 g) were put into a 100 mL flask. The flask was then placed under vacuum and crushed with high purity nitrogen thrice to remove any air. The monomer salts were mechanically stirred and heated to 190 °C under a nitrogen atmosphere for 2 h. Then, the nitrogen flow was

Table 1
The Young's modulus and elongation at break of MWNTs/PA1010 composites made by in situ polymerization and melt-mixing

Sample[a]	MWNTs content (wt%)[b]	Young's modulus (MPa)	Increment (%)[c]	Increment (%)[d]	Elongation at break (%)
LPA1010	0	1021	–	–	37
NTPA-1	1	1301	27.4	8.1	35
NTPA-2	2.5	1302	27.5	8.2	31
NTPA-5	5	1449	41.9	20.4	23
NTPA-10	10	1748	71.2	45.3	17
NTPA-20	20	1813	77.6	50.7	9
NTPA-30	30	1912	87.3	58.9	5
NTPA-5B	5	1226	20.1	1.9	27
NTPA-10B	10	1694	65.9	40.8	19
NTPA-30B	30	1769	73.3	47.0	8

[a] Samples of NTPA-1 to NTPA-30 were made by the in situ polymerization method, and samples of NTPA-5B to NTPA-30B were made by the melt-mixing method.
[b] The content represents the feed weight percentage.
[c] Increment with LPA1010 as the reference, calculated by the equation: Young modulus of (composites-LPA1010)/Young modulus of LPA1010.
[d] Increment with CPA1010 as the reference, calculated by the equation: Young modulus of (composites-CPA1010)/Young modulus of CPA1010.

stopped. The prepolymer was vigorously stirred and reacted under vacuum for 4 h at 225 °C, yielding LPA1010.

2.6. Microscopy characterization

A field emission scanning electron microscope (SEM) (JEOL JSM 6700F) was used to observe the pristine MWNTs and the morphology of the failure surfaces of the MWNTs/PA1010 composites.

2.7. Molecular weight measurement

The molecular weight of LPA1010 was measured by GPC. The sample was acetylated by trifluoroacetic anhydride, and then it was resolved in methylene dichloride. The standard used was nylon 6. According to the GPC measurement, the number-average molecular weight (M_n) and polydispersity index (PDI, M_w/M_n) of LPA1010 was ca. 19,200 and 2.23, respectively.

2.8. Differential scanning calorimetry

The melting points of the polyamide under consideration were measured on Perkin–Elmer Pyris-1 differential scanning calorimeter (DSC) under nitrogen.

2.9. X-ray diffraction

The X-ray diffraction (XRD) patterns were recorded using a Rigaku D/max 2550VB/PC diffractometer with 2D area detector operating at a voltage of 40 kV and a current of 100 mA using Cu Kα radiation, which was equipped with a high temperature attachment. When performing variable temperature WAXD measurements, the sample was placed in a platinum block sample holder and heated at a rate of 10 °C/min to the desired temperature and maintained for 5 min before collecting data with a scanning rate of 6 °C/min.

2.10. Thermal analysis

Thermo gravimetric analysis (TGA) was carried out on Perkin–Elmer TGA 7 type of PE Corporation at a rate of 20 °C/min under nitrogen flow.

2.11. Mechanical property testing

According to the standard ASTM D638 published by USA Material Society, the tensile tests were carried out using an Instron universal material testing system (model 4465) at room temperature with gauge length of 20 mm and crosshead speed of 5 mm/min. Property values reported here represent an average of the results for tests run on at least five specimens.

All film samples with thickness of ca. 2 mm were prepared by melted PA1010 being pressed into a film at ca. 220 °C, 150 bar, then followed by cooling slowly to room temperature (RT). Dynamic mechanical analysis (DMA) was performed on the samples ($20.0\times4.0\times0.2$ mm^3) using DMTA IV type dynamic mechanical analyzer (Rheometric Scientific Co.) under tension film mode in a temperature range of ambient to 200 °C at a frequency of 1 Hz and heating rate of 3 °C/min.

3. Results and discussions

3.1. Mechanical property and reinforcement mechanism

Improving the mechanical strength of materials is a fundamental goal for scientists and engineers alike. Blending pristine CNTs or oxidized CNTs with polymers improves the mechanical strength of materials. This is generally attributed to two main factors: good dispersion of CNTs in the polymer matrix and strong van der waals attraction between the polymer chains and CNTs. It is expected that in situ preparation of nanocomposites will have greater mechanical strength than composites prepared by the blending process due to the better dispersion of CNTs in the polymer and the introduction of covalent linkage between the growing polymer chains and the CNTs.

We prepared six composite samples with various MWNTs additions (1.0–30.0 wt%) by in situ polymerization. The corresponding Young's modulus (E) is summarized in Table 1. The Young's modulus of our lab-synthesized PA1010 (LPA1010) is included for comparison. Increasing the MWNT content from 1.0–30.0 wt% increases the corresponding Young's modulus from 27.4% (1301 MPa) to 87.3% (1912 MPa), respectively (LPA1010 as the reference). The Young's modulus of NTPA-1 (1.0 wt% of MWNTs) is 8.1% higher than that of CPA1010 (commercially purchased PA1010), although the Young's modulus of LPA1010 is much lower than that of CPA1010. This indicates that the in situ polymerization method significantly improves the mechanical strength of composites. Compared with CPA1010, the Young's modulus of in situ composites increases from 8.1 to 58.9% when the MWNTs content increases from 1.0 to 30.0 wt%. Previously, it was reported that the modulus of montmorillonite/PA1010 intercalated composites increased by ca. 34.9% compared with pure PA1010 when the montmorillonite content was 17 wt% [47]. The Young's modulus of MWNTs/PA1010 in situ prepared composites increased by ca. 71.2 and 77.6% when the MWNTs concentration was 10.0 and 20.0 wt%, respectively (LPA1010 as the reference). The Young's modulus of the composites can be further enhanced by increasing the molecular weight of the polymer. This will provide additional improvement in industrial manufacture where high molecular weight can be achieved more easily due to large-scale production.

Two noticeable transition points are observed for composites containing 1.0 and 10.0 wt% MWNTs (the Y_m increased from 0 to 27.4% and 41.9–71.2%, respectively), as shown in Fig. 2. This implies that the Young's modulus increases nonlinearly with the addition of the nanotube fillers. This result is comparable to the reports of Liu [7] and Meincke [48] on MWNTs/PA6 composites prepared by blending MWNTs with polyamide 6, and Zhang's study [47] on montmorillonite/PA1010 composites obtained by intercalation polymerization.

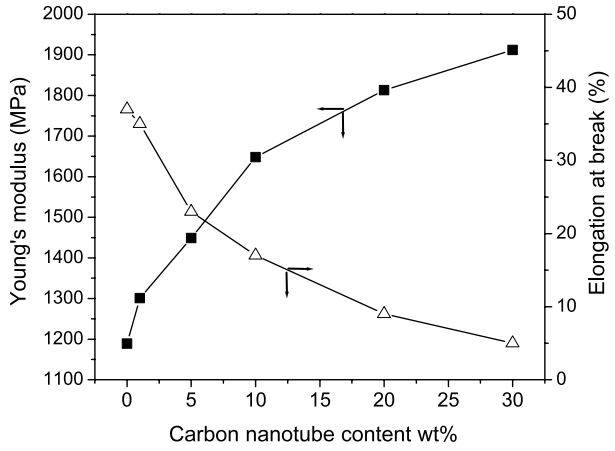

Fig. 2. Young's modulus and elongation at break of MWNTs/PA1010 in situ composites as a function of carbon nanotubes content.

In order to confirm that the in situ polymerization method provides improvement of Young's modulus compared to conventional blending or condensation melt-compounding methods, the blended MWNTs/PA1010 composites were prepared for comparison with the in situ composites. The corresponding Young's modulus values are listed in Table 1. The Young's modulus values of the in situ composites are higher than that of blended composites under the same MWNT–COOH loadings, especially for samples containing 5.0 and 30.0% of nanotubes (i.e. 1449 vs 1226 MPa, and 1912 vs 1769 MPa, respectively). For the MWNTs/PA-6 blended composites with 5.0 and 10.0 wt% MWNTs, the Young's modulus increased by ca. 28.9 and 59.4%, respectively, compared to pure PA6 [48]. For the in situ composites, the Young's modulus increased by ca. 41.9 and 71.2%, (LPA1010 as the reference).

Conversely, CNTs or montmorillonite filler generally makes the composites brittle according to the elongation at break (E_b) test (Fig. 2, Table 1). The E_b decreases proportionately with increasing content of MWNTs, suggesting that the toughness of the in situ composites is influenced by the addition of the nanotube filler. Compared with the montmorillonite filler [47], CNTs demonstrate a greater improvement of mechanical strength in the composites, and a superior ability to maintain the toughness of the original polymer material. The E_b of montmorillonite/PA1010 decreased from 24.0 to 3.0% with increasing montmorillonite content from 0 to 17.0 wt% [47]; while E_b for MWNTs/PA1010 in situ composites only varied from 37.0 to 9.0% at a MWNTs addition of 20.0 wt%. Interestingly, the E_b of MWNTs/PA1010 blended composites is slightly larger than that of in situ composites with the same nanotube loading. This is probably due to the abundant covalent bonds between the CNTs and polymer in the in situ composites, which restricts the stretching and slippage of the polymer chains and tubes. In contrast, the polymer and CNTs in the blended composites have a higher stretching ability due to less covalent bonding caused by macromolecular steric hindrance.

To understand the reinforcing mechanism, the failure surfaces of MWNTs/PA1010 in situ composites after tensile testing were observed by SEM. Fig. 3 shows SEM images of the fracture surfaces of composites containing 5.0 and 30.0 wt% MWNTs. The broken ends of the MWNTs are seen protruding from the polymer matrix and are uniformly dispersed. Individual MWNTs are evenly dispersed throughout the PA1010 matrix when the concentration of MWNTs is as low as 5.0 wt% or as high as 30.0 wt%. The tubes appear bigger than those of crude MWNTs and no hollow structure was found at the broken ends (Fig. 3, images (c) and (d)), which indicates that the nanotubes are wrapped with a layer of polymer. Polymer chains bonded to MWNTs enhances the mixing and dispersion of nanotubes with in situ-formed free polymer. Such covalent linkage is associated with the good dispersion of the nanotube filler in the resulting MWNTs/PA1010 in situ composites, and contributes to the exceptional mechanical

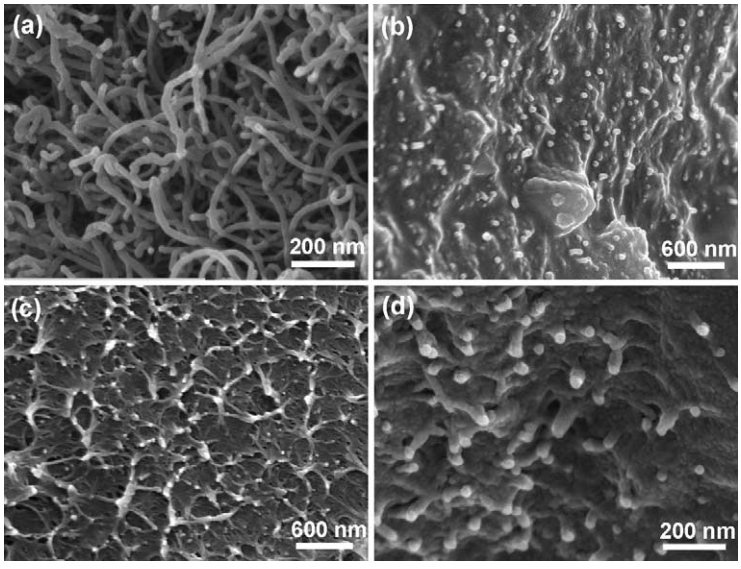

Fig. 3. Typical SEM images of crude MWNTs (a), failure surfaces of NTPA-5 (b) and NTPA-30 (c, d).

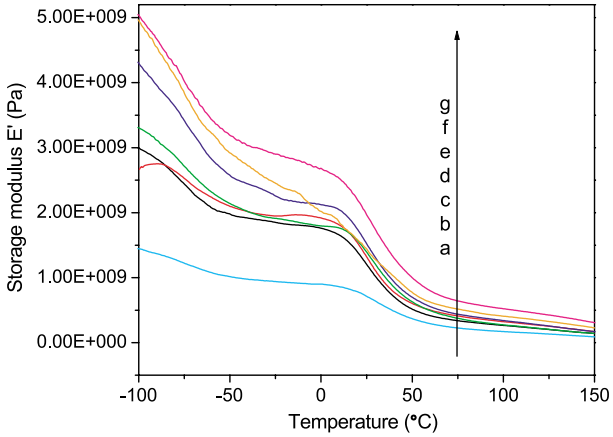

Fig. 4. Storage modulus vs temperature DMA curves for neat PA1010 and its composites: pure LPA1010 (a), NTPA-1 (b), NTPA-2 (c), NTPA-5 (d), NTPA-10 (e), NTPA-20 (f), NTPA-30 (g).

properties observed. Although the tubes are also well dispersed in the blended composites, the mechanical strength was lower than that of the in situ composites due to fewer covalent bonds between the tubes and polymer chains.

3.2. Thermomechanical properties measured by DMA

Fig. 4 shows the storage modulus vs temperature (DMA) curves of various PA1010 composites with different MWNTs additions. The storage modulus of the materials increases significantly upon addition of MWNTs and then further increases gradually as the MWNTs content attains 30.0 wt%. The composite with 1.0 wt% MWNTs addition displays ca. 105% increment of storage modulus (1.85 GPa) as compared with LPA1010 (0.90 GPa) at the glassy plateau region (−25 °C), and ca. 30.0% improvement when compared to the rubbery plateau region (100 °C). For composites with 30.0 wt% MWNTs addition, the storage modulus at −25 °C (2.75 GPa) and 100 °C (0.75 GPa) increases by ca. 198 and 200%, respectively. This pronounced improvement in storage modulus for MWNTs/PA1010 in situ composites can be attributed to the fine dispersion of MWNTs and the covalent linkages between the tubes and polymers. As a comparison, for the MWNTs/PA6 blended composites, storage modulus improvements of 43 and 57% were observed when compared with PA6 at the glassy and rubbery regions [7].

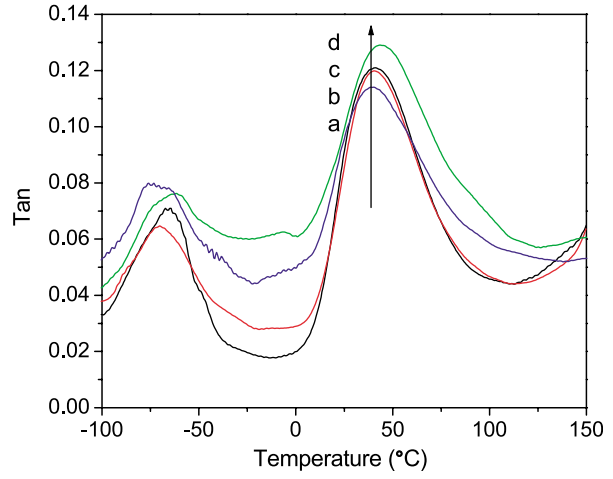

Fig. 5. The tan δ of neat PA1010 and MWNTs/PA1010 in situ composites as a function of temperature: PA1010 (a), NTPA-1 (b), NTPA-10 (c) and NTPA-20 (d).

Fig. 5 shows the tan δ values as a function of temperature for LPA1010 and MWNTs/PA1010 composites. Two loss peaks were observed in the curves. The first at ca. 36–43 °C represents the glass transition temperature (T_g) of the composites, and the second at ca. − 82 to − 65 °C shows relaxation arising from the hydrogen bonds between the nylon polymer chains. As a result of MWNT addition, the two loss peaks transfer toward the higher temperature region with increasing MWNTs content. The relaxation peak at the lower temperature shifts toward the higher temperature peak with increasing MWNT content in the nanocomposites. The covalent bonding and interconnection between PA1010 and MWNTs restricts, to some extent, the movement of the PA1010 chains, which may result in the observed shift of the two loss peaks. Especially, for larger MWNTs loadings, the polymer chains become more restricted, therefore the relaxation peak shifts to higher temperature compared to that of nanocomposites with lower MWNTs content. Conversely, for the MWNTs/PA6 blended composites, the T_g did not change with respect to PA6, due to a lower covalent linkage between MWNTs and PA 6 [7].

3.3. Thermogravimetric analysis

Fig. 6 shows TGA curves for nylon 1010 and PA1010-MWNT in situ composites with MWNT loadings of 5.0, 10.0 and 20.0 wt%. The onset temperature for thermal degradation of PA1010 increases proportionally with the incorporation of MWNTs. The PA1010 macromolecular chains are intensely interconnected with MWNTs, and since polymer thermal degradation begins with chain cleavage and radical formation, the MWNTs in the composite act as radical scavengers, delaying the onset of thermal degradation and hence improves the thermal stability of PA1010 [49].

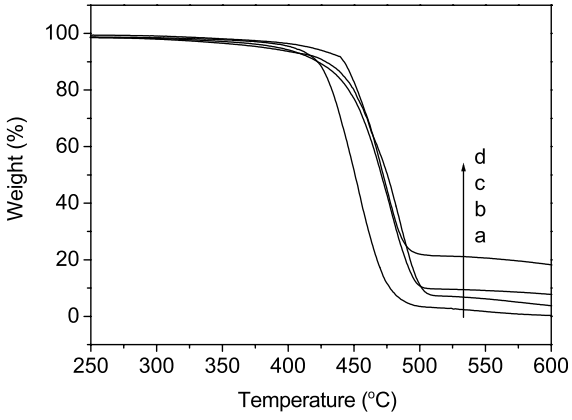

Fig. 6. TGA curves of neat nylon 1010 (a) and the nylon 1010-MWNTs in situ nanocomposites with MWNT content of 5 wt% (b), 10 wt% (c) and 20 wt% (d).

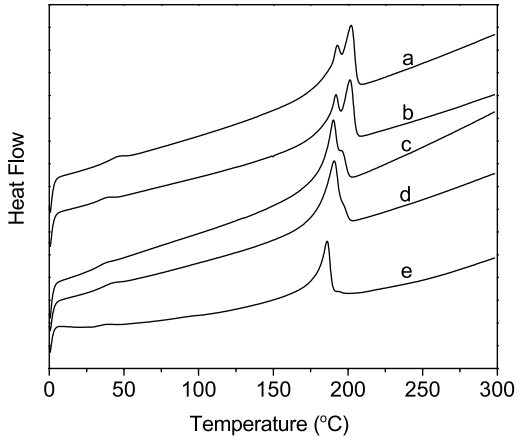

Fig. 7. DSC heating thermograms of PA1010 (a) and MWNTs/PA1010 in situ composites with MWNTs content of 1 wt% (b), 5 wt% (c), 10 wt% (d) and 30 wt% (e).

3.4. Melting and crystallization properties measured by DSC

The crystal form has influence on the mechanical property of the composites. Therefore, in order to gain a greater understanding for the high mechanical strength of the in situ composites, their melting and crystallization behaviors were investigated by DSC and XRD. Fig. 7 shows the DSC heating thermo grams of LPA1010 and the in situ composites. The samples were heated from RT to 300 °C at 20 °C/min. The melting temperature (T_m) of the composites decreased uniformly with increasing MWNT content, indicating that the molecular weight of the polymer decreases with increasing MWNT content due to premature end-capping of active terminals during the in situ formation of the polymer. Double melting peaks were observed in the curves of pure LPA1010 and MWNTs/PA1010 composites with MWNTs contents $<$ 5.0 wt%. The higher temperature peak deceased with increasing MWNTs content, and disappeared when the MWNT content reached 30.0 wt%. Double melting peaks are a universal phenomenon which occurs during the melting process of pure PA1010 and results from the PA1010 melt recrystallization [43–45]. It was reported that the lower temperature peak corresponds to crystal melting at the different crystallizing temperatures, and the higher temperature peak corresponds to the melting of the recrystalised polymer. For the composites, the higher temperature peak intensity decreases and then disappears, implying that the melting of the recrystallised polymer becomes more difficult as the MWNTs content increases. This may be due to polymer chains bonded to the surface of the nanotubes, resulting in restricted movement and re-arrangement of the chains in the composites with higher MWNT loadings. Alternatively, the MWNTs in the composites can be viewed as crystal nuclei and therefore induce a suppression of the melting point with increasing tube content. This provides further evidence that the MWNTs are dispersed uniformly in the composites.

In order to get more information about the difference between pure nylon 1010 and the in situ composites, non-isothermal crystallization behaviors for LPA1010 and nylon 1010/MWNTs (5.0 wt%) nanocomposites at various cooling rates were investigated by DSC. The samples were heated from RT to 230 °C, and maintained at this temperature for 10 min; and then cooled from 230 °C to RT at 5, 10, 20 and 40 °C/min, respectively. Fig. 8 shows the DSC thermogram curve for LPA1010 (A) and nanocomposites with 5.0 wt% of MWNTs (B) at the various cooling rates. The corresponding peak temperature (T_p), initial temperature (T_i) and end temperature (T_e) of crystallization are listed in Table 2. The crystallization peaks of two samples move to a lower temperature with the cooling rate increasing. As the cooling rate increases, the movement of the nylon 1010 macromolecules cannot match the change of the cooling rate. This is called the hysteresis effect. At the same cooling rate, the crystallization peak of the composites (Fig. 8(B)) is sharper than that of LPA1010 (Fig. 8(A)), indicating that the addition of MWNTs noticeably accelerates the crystallization of nylon 1010 polymer chains. On the other hand, strong interactions between the MWNTs and PA1010 chains lead to PA1010 in nanocomposites crystallizing at a higher temperature compared with pure nylon 1010 (Fig. 8 and Table 2). This data implies that MWNTs accelerate the crystallization of polymer in nanocomposites. However, the ΔH_c value of nanocomposites is lower than that of pure nylon 1010 at the same crystallization conditions. This can be explained by the fact that the addition of carbon nanotubes enhances crystallization of the nanocomposites, and reduces the molecular chain movement at the same time. Therefore, the degree of crystallization for the nanocomposites decreases compared with pure PA1010. Double crystal peaks in Fig. 8(A) shows that the LPA1010 was not affected by the rate of crystallization, which could be induced by crystal nuclei. Compared with LPA1010, the MWNTs in the nanocomposites can act a crystal nucleus, therefore the nanocomposites have only one crystal peak.

Table 2
Values of T_i, T_p, T_e and ΔH_c measured by DSC at various cooling rate for nylon 1010, nylon 1010/MWNTs nanocomposites with 5 wt% MWNT

Sample	Φ (°C/min)	T_i (°C)	T_p (°C)	T_e (°C)	ΔH_c (J/g)
LPA1010	5	179.977	178.354	176.307	37.442
	10	177.848	175.496	172.144	42.439
	20	175.121	171.516	166.721	45.730
	40	170.668	165.496	157.184	49.875
NTPA-5	5	181.218	179.042	177.111	37.012
	10	179.696	177.490	173.489	39.335
	20	177.234	173.277	168.762	44.049
	40	174.651	170.200	162.464	45.925

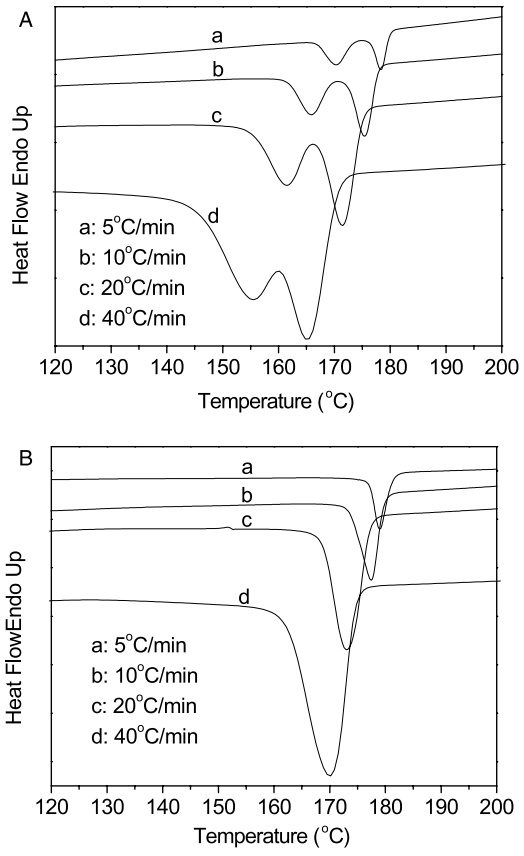

Fig. 8. DSC thermograms of non-isothermal crystallization for nylon 1010 (A) and nylon 1010/MWNTs (5 wt%) nanocomposites (B) at various cooling rates.

Fig. 8(A) shows that the molecular chains in pure nylon 1010 have significant motion in the high temperature range unlike that of the MWNT composites, in which the MWNTs restrict or block the movement of nylon 1010 polymer chains.

We conclude that the improvement of the mechanical properties for the nanocomposites is not due to the effect of the MWNTs on the crystallization of the polymer, therefore the MWNTs independently enforces the nylon 1010 matrix.

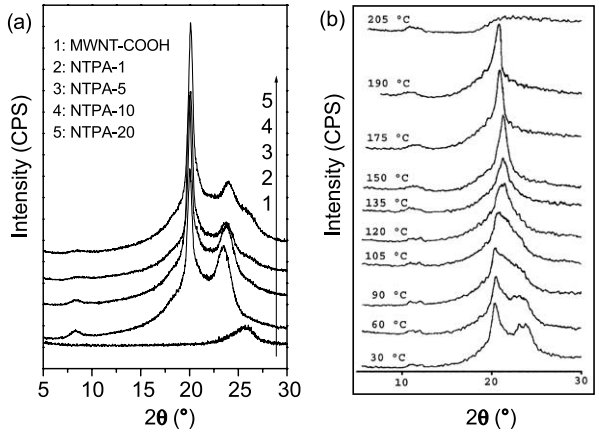

Fig. 9. (a) WAXD patterns of MWNT-COOH (1), NTPA-1(2), NTPA-5 (3), NTPA-10 (4) and NTPA-20 (5) at room temperature. (b) Variable-temperature WAXD patterns of neat PA1010.

3.5. Crystalline transition by XRD

Generally, polyamide can be resolved into α- or γ-forms [50]. In the wide-angle X-ray diffraction (WAXD) pattern, the α-form crystal belongs to the triclinic system characteristic of two strong diffraction signals at $2\theta = 20$ and 24° (100 and 010/110 reflections). The γ-form for PA1010 is observed as a strong peak about $2\theta = 22°$ [51]. Fig. 9 shows the WAXD patterns of MWNT–COOH and MWNTs/PA1010 in situ nanocomposites. The WAXD patterns of MWNTs/PA1010 (pattern 2–5 in Fig. 9) reveal two peaks at about $2\theta = 20$ and 24°, indicating that all the composites present only the α-form structure in our experimental conditions. In contrast, the γ-form (diffraction peak ca. $2\theta = 22°$ at RT) was clearly observed for montmorillonite/PA1010 composites [52]. The authors [52] suggested that the addition of montmorillonite induces or/and stabilizes the γ-crystalline form of PA1010 because the two-dimensional (2D) montmorillonite sheets can disrupt the α-crystallite formation and facilitate the formation of less ordered γ-crystals. Alternatively, our observation is very similar to Liu's [7] report on MWNTs/PA6 blended composites, in which the γ-phase crystals of nylon 6 were not observed yet. We postulate that the 1D nanotubes can act as the nucleation sites and hence encourage α-phase formation. These details are currently under investigation.

Fig. 10 represents the XRD of MWNTs/PA1010 in situ composites with different MWNTs contents (5, 10 and 20 wt%), heating from RT until the nanocomposites melted. Only two peaks were observed at about $2\theta = 20$ and 24° (assigned to the α-crystal), for the MWNTs-reinforced in situ composites. As the temperature increases and reaches melting point, the two peaks gradually move toward each other but do not converge into one peak. There is only one broad brimmed peak when the temperature increases to ca. 182–190 °C. As a comparison, XRD pattern of pure PA1010 was displayed herein (Fig. 9(b)) [53]. It is found that the two diffractions at ca. $2\theta = 20$ and 24° approach to each other gradually as temperature increases and merge into one strong diffraction at ca. $2\theta = 22°$ at ca. 150 °C. This indicated that the crystal-to-crystal transition, from the α-form structure at room temperature to the pseudo-hexagonal lattice at high temperature, occurs in the heating process of neat PA1010. This phenomenon is termed a 'Brill transition', which was discovered for nylon 66 by Brill in 1942 [50] and can be easily observed for many even-even nylons during the heating process [54]. The reason of the 'Brill transition' is due to 'local melting' [55–60] of the methylene sequences between amido groups [54]. The hydrogen bonds remain intact during this crystalline transition [61]. However, for the MWNTs/PA1010 in situ composites, the 'Brill transition' is not found during the heating process. It is proposed that the carbon nanotubes are homogeneously dispersed throughout the matrix, and the PA1010 molecules arrange and crystallize around MWNTs. Therefore, compared with the pure PA1010, the small and

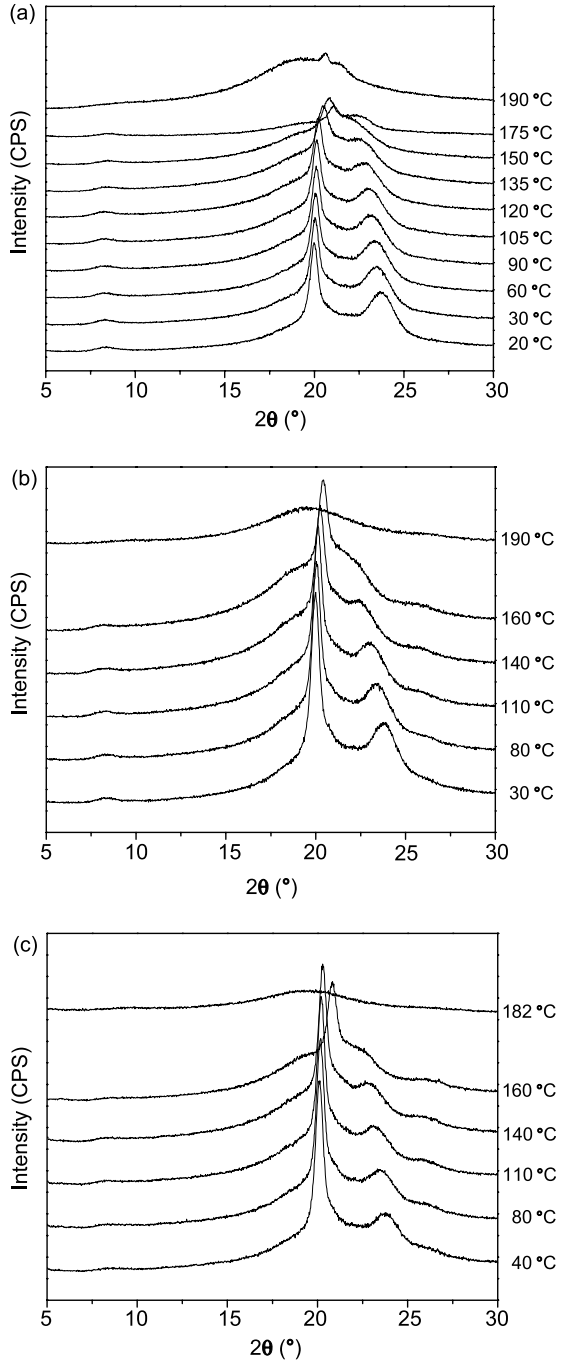

Fig. 10. Variable-temperature WAXD patterns of NTPA-5 (a), NTPA-10 (b), and NTPA-20 (c).

irregular crystals can be formed and hydrogen bonds between the neighboring molecular chains are twisted and become weaker due to the existence of the MWNTs. During the heating process, the methylene sequences between the amido groups become increasingly mobile. At the same time, the weak hydrogen bonds break up, leading to the melting of the MWNTs/PA1010 in situ composites. Thus, the two peaks disappeared simultaneously until the melting point is reached. This suggests that the addition of MWNTs cannot induce such a Brill transition.

4. Conclusions

The MWNT-reinforced PA1010 composites have excellent mechanical properties and were successfully prepared by an in situ polymerization method. Mechanical tests on the composites show that the Young's modulus increases with the addition of MWNTs. The Young's modulus of PA1010 can be improved by 87.3% at a MWNT content of 30.0 wt%. The elongation at break, an indicator of material toughness, decreases (ca. 110%) when MWNTs are incorporated into the PA1010 matrix. Thermogravimetric analysis shows that the onset temperature of thermal degradation for the composites increases with the addition of MWNTs. SEM indicates a uniform dispersion of MWNTs throughout the PA1010 matrix and strong interfacial adhesion between the nanotubes and the polymer. DSC and XRD results show that the effect of MWNTs addition on the melting and crystallization behaviors of nylon 1010 is quite different from that of nylon 1010-montmorillonite composites, probably due to the difference in geometry or morphology of nanofillers.

Acknowledgements

We acknowledge the financial supports from the National Natural Science Foundation of China (Nos 50473010 and 20304007), Fok Ying Tung Education Foundation (No. 91013), Rising-Star Program Foundation of Shanghai (No. 03QB14028), the Opening Research Foundation of the Key Laboratory of Molecular Engineering of Polymers of Ministry of Education in Fudan University and EPSRC.

References

[1] (a) Iijima S. Nature (London) 1991;354:56.
(b) Iijima S, Ichihashi T. Nature (London) 1993;363:603.
[2] (a) Dalton AB, Collins S, Razal J, Munoz E, Ebron VH, Kim BG, et al. J Mater Chem 2004;14:1.
(b) Dalton AB, Collins S, Munoz E, Razal JM, Ebron VH, Ferraris JP, et al. Nature (London) 2003;423:703.
[3] Qian D, Dickey EC, Andrews R, Rantell T. Appl Phys Lett 2000;76:2868.
[4] Sabba Y, Thomas EL. Macromolecules 2004;37:4815.
[5] Lin Y, Zhou B, Fernando KAS, Liu P, Allard LF, Sun YP. Macromolecules 2003;36:7199.
[6] Sandler J, Shaffer MSP, Prasse T, Bauhofer W, Schulte K, et al. Polymer 1999;40:5967.
[7] Liu TX, Phang IY, Shen L, Chow SY, Zhang WD. Macromolecules 2004; 37:7214.
[8] (a) Tong Y, He XJ, Cheng HM. New Carbon Mater 2004;19:261.
(b) Tang WZ, Santare MH, Advani SG. Carbon 2003;41:2779.
[9] Potschke P, Fornes TD, Paul DR. Polymer 2002;43:3247.
[10] Andrews R, Jacques D, Minot M, Randell T. Macromol Mater Eng 2002; 287:395.
[11] Jin ZX, Pramoda KP, Xu GQ, Goh SH. Chem Phys Lett 2001;337:43.
[12] Dang ZM, Fan LZ, Shen Y, Nan CW. Mater Sci Eng B, Solid-State Mater Adv Tech 2003;103(40):140.
[13] Fan JH, Wan MX, Zhu DB, Chang BH, Pan ZW, Xie SS. Synth Met 1999; 102:1266.
[14] Philip B, Xie JN, Abraham JK, Varadan VK. Polym Bull 2005;53:127.
[15] Shaffer MSP, Koziol K. Chem Commun 2002;2074.
[16] Viswanathan G, Chakrapani N, Yang HC, Wei BQ, Chung HS, Cho KW, et al. J Am Chem Soc 2003;125:9258.

[17] Kong H, Gao C, Yan DY. J Am Chem Soc 2004;126:412.
[18] Qu LW, Lin Y, Hill DE, Zhou B, Wang W, Sun XF, et al. Macromolecules 2004;37:6055.
[19] Lin Y, Zhou B, Fernando KAS, Liu P, Allard LF, Sun YP. Macromolecules 2003;36:7199.
[20] Zhao B, Hu H, Haddon RC. Adv Fun Mater 2004;14:71.
[21] (a) Qin SH, Qin DQ, Ford WT, Herrera JE, Resasco DE, Bachilo SM, et al. Macromolecules 2004;37:3965–7.
(b) Kong H, Luo P, Gao C, Yan DY. Polymer 2005;46:2472.
[22] (a) Kong H, Li W, Gao C, Yan D, Jin YZ, Walton DRM, et al. Macromolecules 2004;37:6683.
(b) Sun T, Liu H, Song W, Wang X, Jiang L, Li L, et al. Angew Chem Int Ed 2004;43:4663.
[23] Qin SH, Qin DQ, Ford WT, Herrera JE, Resasco DE. Macromolecules 2004;37:9963.
[24] Wu W, Zhang S, Li Y, Li JX, Liu LQ, Qin YJ, et al. Macromolecules 2003;36:6286.
[25] Xu YY, Gao C, Kong H, Yan DY, Jin YZ, Watts PCP. Macromolecules 2004;37:8846.
[26] Cao L, Yang W, Yang J, Wang C, Fu S. Chem Lett 2004;33:490.
[27] (a) Sun YP, Huang W, Carroll DL. Chem Mater 2001;13:2864.
(b) Fu K, Huang W, Lin Y, Riddle LA, Carroll DL, Sun YP. Nano Lett 2001;1:439.
[28] Zheng M, Jagota A, Semke ED, Diner BA, Mclean RS, Lustig SR, et al. Nature Mater 2003;2:338.
[29] Endo M, Takeuchi K, Hiraoka T, Furuta T, Kasai T, Sun X, et al. J Phys Chem Solids 1997;58:1707.
[30] Rochefort A. Phys Rev B 2003;67:115401.
[31] Gomez FJ, Chen RJ, Wang DW, Waymouth RM, Dai HJ. Chem Commun 2003;(2):190.
[32] Chen CW, Lee MH, Clark SJ. App Surf Sci 2004;228:143.
[33] Stafstrom S, Hansson A, Johansson A. Synth Met 2003;137:1397.
[34] Fukushima T, Kosaka A, Ishimura Y, Yamamoto T, Takigawa T, Ishii N, et al. Science 2003;300:2072.
[35] Yang C, Wohlgenannt M, Vardeny ZV, Blau WJ, Dalton AB, Baughman R, et al. Physica B-Condens Matter 2003;338:366.
[36] Yang X, Chen L, Shuai Z, Liu Y, Zhu D. Adv Fun Mater 2004;14:289.
[37] Sangoi R, Fuller L, Santhanam KSV. Mater Res Soc Symp Proc 2003; 788:191.
[38] Steuerman DW, Star A, Narizzano R, Choi H, Ries RS, Nicolini C, et al. J Phys Chem B 2002;106:3124.
[39] Zhu ZP, Su DS, Weinberg G, Schlogl R. Nano Lett 2004;4:2255.
[40] Richard C, Balavoine F, Schultz P, Ebbesen TW, Mioskowski C. Science 2003;300:775.
[41] Jia Z, Xu C, Liang J, Wei B, Wu D, Zhu C. Xinxing Tan Cailiao 1999;14: 32.
[42] Jia Z, Wang Z, Xu C, Liang J, Wei B, Wu D, Zhang Z. Qinghua Daxue Xuebao. Ziran Kexueban 2000;40:14.
[43] Philip B, Xie J, Chandrasekhar A, Abraham J, Varadan VK. Smart Mater Struct 2004;13:295.
[44] Zeng FD, Li ZB. J Fun Mater 2004;35:2670.
[45] Mo Z, Meng Q, Feng J. Polym Inter 1993;32:53.
[46] (a) Gao C, Vo CD, Jin YZ, Li WW, Armes SP. Macromolecules 2005;38: 8634.
(b) Liu J, Rinzler AG, Dai HJ, Hafner JH, Bradley RK, Boul PJ, et al. Science 1998;280:1253.
[47] Zhang GS. Doctoral Dissertation of Shanghai Jiaotong University; 2003 p. 82.
[48] Meincke O, Kaempfer D, Weickmann H, Friedrich C, Vathauer M, Warth H. Polymer 2004;45:739.
[49] Watts PCP, Fearon PK, Hsu WK, Billingham NC, Kroto HW, Walton DRM. J Mater Chem 2003;13:491.
[50] Brill R. J Prakt Chem 1942;161:46.
[51] Li YJ, Yan DY, Zhu XY. Macromol Rapid Commun 2000;21:282.
[52] Zhang GS, Li YJ, Yan DY. Polym Inter 2003;52:795.
[53] Li YJ. Doctoral Dissertation of Shanghai Jiao Tong University; 2001 p. 53,55.
[54] Yan DY, Li YJ, Zhu XY. Macromol Rapid Commun 2000;21:1040.
[55] Itoh T. Jpn J Appl Phys 1976;15:2295.
[56] Starkweather Jr HW, Jones GA. J Polym Sci. Polym Phys 1981;19:467.
[57] Hirschinger J, Miura H, Gardner KH, English AD. Macromolecules 1990; 23:2153.
[58] Lovinger AJ. J Appl Phys 1978;49:5003.
[59] Murthy NS, Curran SA, Aharoni SM, Minor H. Macromolecules 1991;24: 3215.
[60] Biangardi HJ. J Macromol Sci Phys 1990;B29(2–3):139.
[61] Cui XW, Li WH, Yan DY. Polym Inter 2004;53:2031.